Hindawi Publishing Corporation
EURASIP Journal on Wireless Communications and Networking
Volume 2007, Article ID 19070, 19 pages
doi:10.1155/2007/19070

Research Article

Survey of Channel and Radio Propagation Models for Wireless MIMO Systems

P. Almers,[1] E. Bonek,[2] A. Burr,[3] N. Czink,[2,4] M. Debbah,[5] V. Degli-Esposti,[6] H. Hofstetter,[5] P. Kyösti,[7] D. Laurenson,[8] G. Matz,[2] A. F. Molisch,[9,1] C. Oestges,[10] and H. Özcelik[2]

[1] *Department of Electroscience, Lund University, P.O. Box 118, 221 00 Lund, Sweden*
[2] *Institut für Nachrichtentechnik und Hochfrequenztechnik, Technische Universität Wien, Gußhausstraße, 1040 Wien, Austria*
[3] *Department of Electronics, University of York, Heslington, York YO10 5DD, UK*
[4] *Forschungszentrum Telekommunikation Wien (ftw.), Donau City Straße 1, 1220 Wien, Austria*
[5] *Mobile Communications Group, Institut Eurecom, 2229 Route des Cretes, BP193, 06904 Sophia Antipolis, France*
[6] *Dipartimento di Elettronica, Informatica e Sistemistica, Università di Bologna, Villa Griffone, 40044 Pontecchio Marconi, Bologna, Italy*
[7] *Elektrobit, Tutkijantie 7, 90570 Oulu, Finland*
[8] *Institute for Digital Communications, School of Engineering and Electronics, The University of Edinburgh, Mayfield Road, Edinburgh EH9 3JL, UK*
[9] *Mitsubishi Electric Research Lab, 558 Central Avenue, Murray Hill, NJ 07974, USA*
[10] *Microwave Laboratory, Universite catholique de Louvain, 1348 Louvain-la-Neuve, Belgium*

Received 24 May 2006; Revised 15 November 2006; Accepted 15 November 2006

Recommended by Rodney A. Kennedy

This paper provides an overview of the state-of-the-art radio propagation and channel models for wireless multiple-input multiple-output (MIMO) systems. We distinguish between *physical models* and *analytical models* and discuss popular examples from both model types. Physical models focus on the double-directional propagation mechanisms between the location of transmitter and receiver without taking the antenna configuration into account. Analytical models capture physical wave propagation and antenna configuration simultaneously by describing the impulse response (equivalently, the transfer function) between the antenna arrays at both link ends. We also review some MIMO models that are included in current standardization activities for the purpose of reproducible and comparable MIMO system evaluations. Finally, we describe a couple of key features of channels and radio propagation which are not sufficiently included in current MIMO models.

1. INTRODUCTION AND OVERVIEW

Within roughly ten years, multiple-input multiple-output (MIMO) technology has made its way from purely theoretical performance analyses that promised enormous capacity gains [1, 2] to actual products for the wireless market (e.g., [3–6]). However, numerous MIMO techniques still have not been sufficiently tested under realistic propagation conditions and hence their integration into real applications can be considered to be still in its infancy. This fact underlines the importance of physically meaningful yet easy-to-use methods to understand and mimic the wireless channel and the underlying radio propagation [7]. Hence, the modeling of MIMO radio channels has attracted much attention.

Initially, the most commonly used MIMO model was a spatially i.i.d. flat-fading channel. This corresponds to a so-called "rich scattering" narrowband scenario. It was soon realized, however, that many propagation environments result in spatial correlation. At the same time, interest in wideband systems made it necessary to incorporate frequency selectivity. Since then, more and more sophisticated models for MIMO channels and propagation have been proposed.

This paper provides a survey of the most important developments in the area of MIMO channel modeling. We classify the approaches presented into *physical models* (discussed in Section 2) and *analytical models* (Section 3). Then, MIMO models developed within wireless standards are reviewed in Section 4 and finally, a number of important aspects lacking in current models are discussed (Section 5).

1.1. Notation

We briefly summarize the notation used throughout the paper. We use boldface characters for matrices (upper case) and vectors (lower case). Superscripts $(\cdot)^T$, $(\cdot)^H$, and $(\cdot)^*$ denote transposition, Hermitian transposition, and complex conjugation, respectively. Expectation (ensemble averaging) is denoted $E\{\cdot\}$. The trace, determinant, and Frobenius norm of a matrix are written as $\mathrm{tr}\{\cdot\}$, $\det\{\cdot\}$, and $\|\cdot\|_F$, respectively. The Kronecker product, Schur-Hadamard product, and vectorization operation are denoted $\otimes$, $\odot$, and $\mathrm{vec}\{\cdot\}$, respectively. Finally, $\delta(\cdot)$ is the Dirac delta function and $\mathbf{I}_n$ is the $n \times n$ identity matrix.

1.2. Previous work

An introduction to wireless communications and channel modeling is offered in [8]. The book gives a good overview about propagation processes, and large- and small-scale effects, but without touching multiantenna modeling.

A comprehensive introduction to wireless channel modeling is provided in [7]. Propagation phenomena, the statistical description of the wireless channel, as well as directional MIMO channel characterization and modeling concepts are presented.

Another general introduction to space-time communications and channels can be found in [9], though the book concentrates more on MIMO transmitter and receiver algorithms.

A very detailed overview on propagation modeling with focus on MIMO channel modeling is presented in [10]. The authors give an exclusive summary of concepts, models, measurements, parameterization and validation results from research conducted within the COST 273 framework [11].

1.3. MIMO system model

In this section, we first discuss the characterization of wireless channels from a propagation point of view in terms of the double-directional impulse response. Then, the system level perspective of MIMO channels is discussed. We will show how these two approaches can be brought together. Later in the paper we will distinguish between "physical" and "analytical" models for characterization purposes.

1.3.1. Double-directional radio propagation

In wireless communications, the mechanisms of radio propagation are subsumed into the impulse response of the channel between the position $\mathbf{r}_{\mathrm{Tx}}$ of the transmitter (Tx) and the position $\mathbf{r}_{\mathrm{Rx}}$ of the receiver (Rx). With the assumption of ideal omnidirectional antennas, the impulse response consists of contributions of all individual multipath components (MPCs). Disregarding polarization for the moment, the temporal and angular dispersion effects of a static (time-invariant) channel are described by the *double-directional* channel impulse response [12–15]

$$h(\mathbf{r}_{\mathrm{Tx}}, \mathbf{r}_{\mathrm{Rx}}, \tau, \phi, \psi) = \sum_{l=1}^{L} h_l(\mathbf{r}_{\mathrm{Tx}}, \mathbf{r}_{\mathrm{Rx}}, \tau, \phi, \psi). \tag{1}$$

Here, τ, ϕ, and ψ denote the excess delay, the direction of departure (DoD), and the direction of arrival (DoA), respectively.[1] Furthermore, L is the total number of MPCs (typically those above the noise level of the system considered). For planar waves, the contribution of the lth MPC, denoted $h_l(\mathbf{r}_{\mathrm{Tx}}, \mathbf{r}_{\mathrm{Rx}}, \tau, \phi, \psi)$, equals

$$h_l(\mathbf{r}_{\mathrm{Tx}}, \mathbf{r}_{\mathrm{Rx}}, \tau, \phi, \psi) = a_l \delta(\tau - \tau_l)\delta(\phi - \phi_l)\delta(\psi - \psi_l), \tag{2}$$

with a_l, τ_l, ϕ_l, and ψ_l denoting the complex amplitude, delay, DoD, and DoA, respectively, associated with the lth MPC. Nonplanar waves can be modeled by replacing the Dirac deltas in (2) with other appropriately chosen functions[2] (e.g., see [16]).

For *time-variant* (nonstatic) channels, the MPC parameters in (2) $(a_l, \tau_l, \phi_l, \psi_l)$ the Tx and Rx position $(\mathbf{r}_{\mathrm{Tx}}, \mathbf{r}_{\mathrm{Rx}})$, and the number of MPCs (L) may become functions of time t. We then replace (1) by the more general *time-variant* double-directional channel impulse response

$$h(\mathbf{r}_{\mathrm{Tx}}, \mathbf{r}_{\mathrm{Rx}}, t, \tau, \phi, \psi) = \sum_{l=1}^{L} h_l(\mathbf{r}_{\mathrm{Tx}}, \mathbf{r}_{\mathrm{Rx}}, t, \tau, \phi, \psi). \tag{3}$$

Polarization can be taken into account by extending the impulse response to a polarimetric (2×2) matrix [17] that describes the coupling between vertical (V) and horizontal (H) polarizations[3]:

$$\mathbf{H}_{\mathrm{pol}}(\mathbf{r}_{\mathrm{Tx}}, \mathbf{r}_{\mathrm{Rx}}, t, \tau, \phi, \psi) = \begin{pmatrix} h^{\mathrm{VV}}(\mathbf{r}_{\mathrm{Tx}}, \mathbf{r}_{\mathrm{Rx}}, t, \tau, \phi, \psi) & h^{\mathrm{VH}}(\mathbf{r}_{\mathrm{Tx}}, \mathbf{r}_{\mathrm{Rx}}, t, \tau, \phi, \psi) \\ h^{\mathrm{HV}}(\mathbf{r}_{\mathrm{Tx}}, \mathbf{r}_{\mathrm{Rx}}, t, \tau, \phi, \psi) & h^{\mathrm{HH}}(\mathbf{r}_{\mathrm{Tx}}, \mathbf{r}_{\mathrm{Rx}}, t, \tau, \phi, \psi) \end{pmatrix}. \tag{4}$$

We note that even for single antenna systems, dual-polarization results in a 2×2 MIMO system. In terms of plane wave MPCs, we have

$$\mathbf{H}_{\mathrm{pol}}(\mathbf{r}_{\mathrm{Tx}}, \mathbf{r}_{\mathrm{Rx}}, t, \tau, \phi, \psi) = \sum_{l=1}^{L} \mathbf{H}_{\mathrm{pol},l}(\mathbf{r}_{\mathrm{Tx}}, \mathbf{r}_{\mathrm{Rx}}, t, \tau, \phi, \psi) \tag{5}$$

[1] DoA and DoD are to be understood as spatial angles that correspond to a point on the unit sphere and replace the spherical azimuth and elevation angles.

[2] Since Maxwell's equations are linear, nonplanar waves can alternatively be broken down into a linear superposition of (infinite) plane waves. However, because of receiver noise it is sufficient to characterize the channel by a finite number of waves.

[3] The V and H polarization are sufficient for the characterization of the far field.

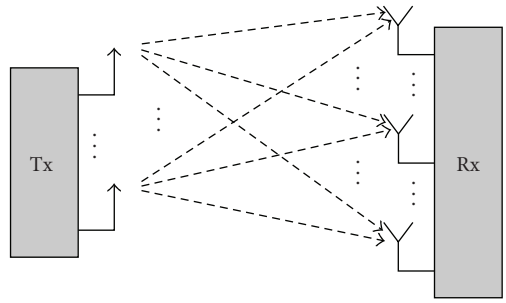

Figure 1: Schematic illustration of a MIMO system with multiple transmit and receive antennas.

with

$$\mathbf{H}_{\mathrm{pol},l}(\mathbf{r}_{\mathrm{Tx}},\mathbf{r}_{\mathrm{Rx}},t,\tau,\phi,\psi) = \begin{pmatrix} a_l^{\mathrm{VV}} & a_l^{\mathrm{VH}} \\ a_l^{\mathrm{HV}} & a_l^{\mathrm{HH}} \end{pmatrix} \delta(\tau-\tau_l)\delta(\phi-\phi_l)\delta(\psi-\psi_l). \quad (6)$$

Here, the "complex amplitude" is itself a polarimetric matrix that accounts for scatterer[4] reflectivity and depolarization. We emphasize that the double-directional impulse response describes only the propagation channel and is thus completely independent of antenna type and configuration, system bandwidth, or pulse shaping.

1.3.2. MIMO channel

In contrast to conventional communication systems with one transmit and one receive antenna, MIMO systems are equipped with multiple antennas at both link ends (see Figure 1). As a consequence, the MIMO channel has to be described for all transmit and receive antenna pairs. Let us consider an $n \times m$ MIMO system, where m and n are the number of transmit and receive antennas, respectively. From a system level perspective, a linear time-variant MIMO channel is then represented by an $n \times m$ channel matrix

$$\mathbf{H}(t,\tau) = \begin{pmatrix} h_{11}(t,\tau) & h_{12}(t,\tau) & \cdots & h_{1m}(t,\tau) \\ h_{21}(t,\tau) & h_{22}(t,\tau) & \cdots & h_{2m}(t,\tau) \\ \vdots & \vdots & \ddots & \vdots \\ h_{n1}(t,\tau) & h_{n2}(t,\tau) & \cdots & h_{nm}(t,\tau) \end{pmatrix}, \quad (7)$$

where $h_{ij}(t,\tau)$ denotes the time-variant impulse response between the jth transmit antenna and the ith receive antenna. There is no distinction between (spatially) separate antennas and different polarizations of the same antenna. If polarization-diverse antennas are used, each element of the matrix $\mathbf{H}(t,\tau)$ has to be replaced by a polarimetric submatrix, effectively increasing the total number of antennas used in the system.

The channel matrix (7) includes the effects of antennas (type, configuration, etc.) and frequency filtering (bandwidth-dependent). It can be used to formulate an overall MIMO input-output relation between the length-m transmit signal vector $\mathbf{s}(t)$ and the length-n receive signal vector $\mathbf{y}(t)$ as

$$\mathbf{y}(t) = \int_\tau \mathbf{H}(t,\tau)\mathbf{s}(t-\tau)d\tau + \mathbf{n}(t). \quad (8)$$

(Here, $\mathbf{n}(t)$ models noise and interference.)

If the channel is time-invariant, the dependence of the channel matrix on t vanishes (we write $\mathbf{H}(\tau) = \mathbf{H}(t,\tau)$). If the channel furthermore is frequency flat there is just one single tap, which we denote by $\mathbf{H}$. In this case (8) simplifies to

$$\mathbf{y}(t) = \mathbf{H}\mathbf{s}(t) + \mathbf{n}(\mathbf{t}). \quad (9)$$

1.3.3. Relationship

We have just seen two different views of the radio channel: on the one hand the double-directional impulse response that characterizes the physical propagation channel, on the other hand the MIMO channel matrix that describes the channel on a system level including antenna properties and pulse shaping. We next provide a link between these two approaches, disregarding polarization for simplicity. To this end, we need to incorporate the antenna pattern and pulse shaping into the double-directional impulse response. It can then be shown that

$$h_{ij}(t,\tau) = \int_{\tau'}\int_\phi\int_\psi h\left(\mathbf{r}_{\mathrm{Tx}}^{(j)},\mathbf{r}_{\mathrm{Rx}}^{(i)},t,\tau',\phi,\psi\right) \times G_{\mathrm{Tx}}^{(j)}(\phi)G_{\mathrm{Rx}}^{(i)}(\psi)f(\tau-\tau')d\tau'\,d\phi\,d\psi. \quad (10)$$

Here, $\mathbf{r}_{\mathrm{Tx}}^{(j)}$ and $\mathbf{r}_{\mathrm{Rx}}^{(i)}$ are the coordinates of the jth transmit and ith receive antenna, respectively. Furthermore, $G_{\mathrm{Tx}}^{(i)}(\phi)$ and $G_{\mathrm{Rx}}^{(j)}(\psi)$ represent the transmit and receive antenna patterns, respectively, and $f(\tau)$ is the overall impulse response of Tx and Rx antennas and frequency filters.

To determine all entries of the channel matrix $\mathbf{H}(t,\tau)$ via (10), the double-directional impulse response in general must be available for all combinations of transmit and receive antennas. However, under the assumption of planar waves and narrowband arrays this requirement can be significantly relaxed (see, e.g., [19]).

1.4. Model classification

A variety of MIMO channel models, many of them based on measurements, have been reported in the last years. The proposed models can be classified in various ways.

A potential way of distinguishing the individual models is with regard to the type of channel that is being considered,

[4] Throughout this paper, the term scatterer refers to any physical object interacting with the electromagnetic field in the sense of causing reflection, diffraction, attenuation, and so forth. The more precise term "interacting objects" has been used in [17, 18].

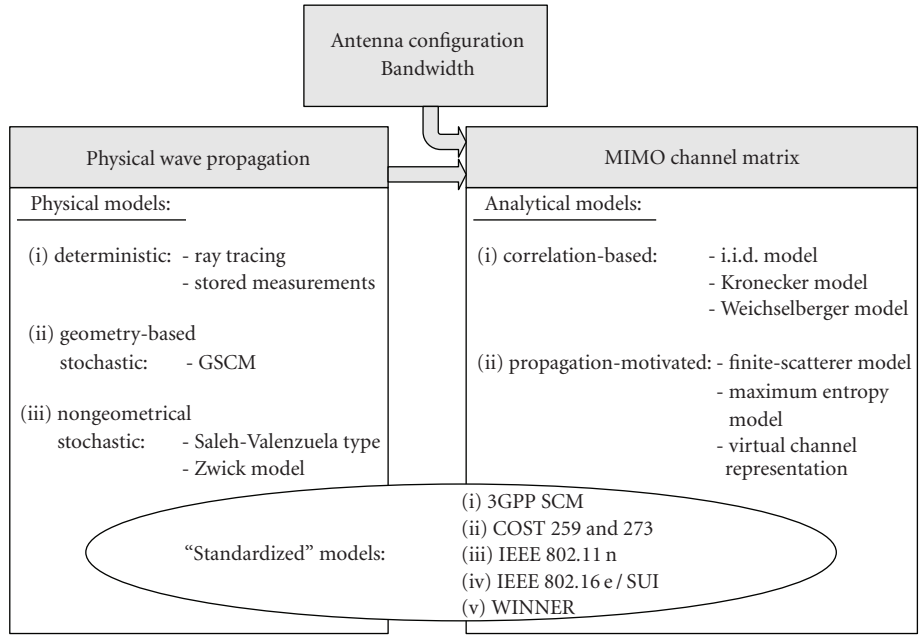

Figure 2: Classification of MIMO channel and propagation models according to [19, Chapter 3.1].

that is, *narrowband* (flat fading) versus *wideband* (frequency-selective) models, *time-varying* versus *time-invariant* models, and so forth. Narrowband MIMO channels are completely characterized in terms of their spatial structure. In contrast, wideband (frequency-selectivity) channels require additional modeling of the multipath channel characteristics. With time-varying channels, one additionally requires a model for the temporal channel evolution according to certain Doppler characteristics.

Hereafter, we will focus on another particularly useful model classification pertaining to the modeling approach taken. An overview of this classification is shown in Figure 2. The fundamental distinction is between *physical models* and *analytical models*. Physical channel models characterize an environment on the basis of electromagnetic wave propagation by describing the double-directional multipath propagation [12, 17] between the location of the transmit (Tx) array and the location of the receive (Rx) array. They explicitly model wave propagation parameters like the complex amplitude, DoD, DoA, and delay of an MPC. More sophisticated models also incorporate polarization and time variation. Depending on the chosen complexity, physical models allow for an accurate reproduction of radio propagation. Physical models are independent of antenna configurations (antenna pattern, number of antennas, array geometry, polarization, mutual coupling) and system bandwidth.

Physical MIMO channel models can further be split into *deterministic models*, *geometry-based stochastic models*, and *nongeometric stochastic models*. Deterministic models characterize the physical propagation parameters in a completely deterministic manner (examples are ray tracing and stored measurement data). With geometry-based stochastic channel models (GSCM), the impulse response is characterized by the laws of wave propagation applied to specific Tx, Rx, and scatterer geometries, which are chosen in a stochastic (random) manner. In contrast, nongeometric stochastic models describe and determine physical parameters (DoD, DoA, delay, etc.) in a completely stochastic way by prescribing underlying probability distribution functions without assuming an underlying geometry (examples are the extensions of the Saleh-Valenzuela model [20, 21]).

In contrast to physical models, analytical channel models characterize the impulse response (equivalently, the transfer function) of the channel between the individual transmit and receive antennas in a mathematical/analytical way without explicitly accounting for wave propagation. The individual impulse responses are subsumed in a (MIMO) channel matrix. Analytical models are very popular for synthesizing MIMO matrices in the context of system and algorithm development and verification.

Analytical models can be further subdivided into *propagation-motivated models* and *correlation-based models*. The first subclass models the channel matrix via propagation parameters. Examples are the finite scatterer model [22], the maximum entropy model [23], and the virtual channel representation [24]. Correlation-based models characterize the MIMO channel matrix statistically in terms of the correlations between the matrix entries. Popular correlation-based analytical channel models are the Kronecker model [25–28] and the Weichselberger model [29].

For the purpose of comparing different MIMO systems and algorithms, various organizations defined reference MIMO channel models which establish reproducible channel conditions. With physical models this means to specify a channel model, reference environments, and parameter values for these environments. With analytical models, parameter sets representative for the target scenarios need to be prescribed.[5] Examples for such reference models are the ones proposed within 3GPP [30], IST-WINNER [31], COST 259 [17, 18], COST 273 [11], IEEE 802.16a,e [32], and IEEE 802.11n [33].

1.5. Stationarity aspects

Stationarity refers to the property that the statistics of the channel are time- (and frequency-) independent, which is important in the context of transceiver designs trying to capitalize on long-term channel properties. Channel stationarity is usually captured via the notion of *wide-sense stationary uncorrelated scattering* (WSSUS) [34, 35]. A dual interpretation of the WSSUS property is in terms of uncorrelated multipath (delay-Doppler) components.

In practice, the WSSUS condition is never satisfied exactly. This can be attributed to distance-dependent path loss, shadowing, delay drift, changing propagation scenario, and so forth that cause nonstationary long-term channel fluctuations. Furthermore, reflections by the same physical object and delay-Doppler leakage due to band- or time-limitations caused by antennas or filters at the Tx/Rx result in correlations between different MPCs. In the MIMO context, the nonstationarity of the spatial channel statistics is of particular interest.

The discrepancy between practical channels and the WSSUS assumption has been previously studied, for example, in [36]. Experimental evidence of non-WSSUS behavior involving correlated scattering has been provided, for example, in [37, 38]. Nonstationarity effects and scatterer (tap) correlation have also found their ways into channel modeling and simulation: see [18] for channel models incorporating large-scale fluctuations and [39] for vector AR channel models capturing tap correlations. A solid theoretical framework for the characterization of non-WSSUS channels has recently been proposed in [40].

In practice, one usually resorts to some kind of quasistationarity assumption, requiring that the channel statistics stay approximately constant within a certain stationarity time and stationarity bandwidth [40]. Assumptions of this type have their roots in the QWSSUS model of [34] and are relevant to a large variety of communication schemes. As an example, consider ergodic MIMO capacity which can only be achieved with signalling schemes that average over many independent channel realizations having the same statistics [41]. For a channel with coherence time T_c and stationarity time T_s, independent realizations occur approximately every T_c seconds and the channel statistics are approximately constant within T_s seconds. Thus, to be able to achieve ergodic capacity, the ratio T_s/T_c has to be sufficiently large. Similar remarks apply to other communication techniques that try to exploit specific long-term channel properties or whose performance depends on the amount of tap correlation (e.g., [42]).

To assess the stationarity time and bandwidth, several approaches have been proposed in the SISO, SIMO, and MIMO context, mostly based on the rate of variation of certain local channel averages. In the context of SISO channels, [43] presents an approach that is based on MUSIC-type wave number spectra (that correspond to specific DOAs) estimated from subsequent virtual antenna array data. The channel non-stationarity is assessed via the amount of change in the wave number power. In contrast, [13, 44] defines stationarity intervals based on the change of the power delay profile (PDP). To this end, empirical correlations of consecutive instantaneous PDP estimates were used. Regarding SIMO channel nonstationarity, [45] studied the variation of the SIMO channel correlation matrix with particular focus on performance metrics relevant in the SIMO context (e.g., beamforming gain). In a similar way, [46] measures the penalty of using outdated channel statistics for spatial processing via a so-called F-eigen ratio, which is particularly relevant for transmissions in a low-rank channel subspace.

The nonstationarity of MIMO channels has recently been investigated in [47]. There, the SISO framework of [40] has been extended to the MIMO case. Furthermore, comprehensive measurement evaluations were performed based on the normalized inner product

$$\frac{\mathrm{tr}\left\{\mathbf{R}_{\mathbf{H}}^{1}\mathbf{R}_{\mathbf{H}}^{2}\right\}}{||\mathbf{R}_{\mathbf{H}}^{1}||_{F}||\mathbf{R}_{\mathbf{H}}^{2}||_{F}} \tag{11}$$

of two spatial channel correlation matrices $\mathbf{R}_{\mathbf{H}}^{1}$ and $\mathbf{R}_{\mathbf{H}}^{2}$ that correspond to different time instants.[6]

This measure ranges from 0 (for channels with orthogonal correlation matrices, that is, completely disjoint spatial characteristics) to 1 (for channels whose correlation matrices are scalar multiples of each other, that is, with identical spatial structure). Thus, this measure can be used to reliably describe the evolution of the long-term spatial channel structure. For the indoor scenarios considered in [47], it was concluded that significant changes of spatial channel statistics can occur even at moderate mobility.

2. PHYSICAL MODELS

2.1. Deterministic physical models

Physical propagation models are termed "deterministic" if they aim at reproducing the actual physical radio propagation process for a given environment. In urban environments, the geometric and electromagnetic characteristics of

[5] Some reference models offer both concepts; they specify the geometric properties of the scatterers using a physical model, but they also provide an analytical model derived from the physical one for easier implementation, if needed.

[6] Of course these correlation matrices have to be estimated over sufficiently short time periods.

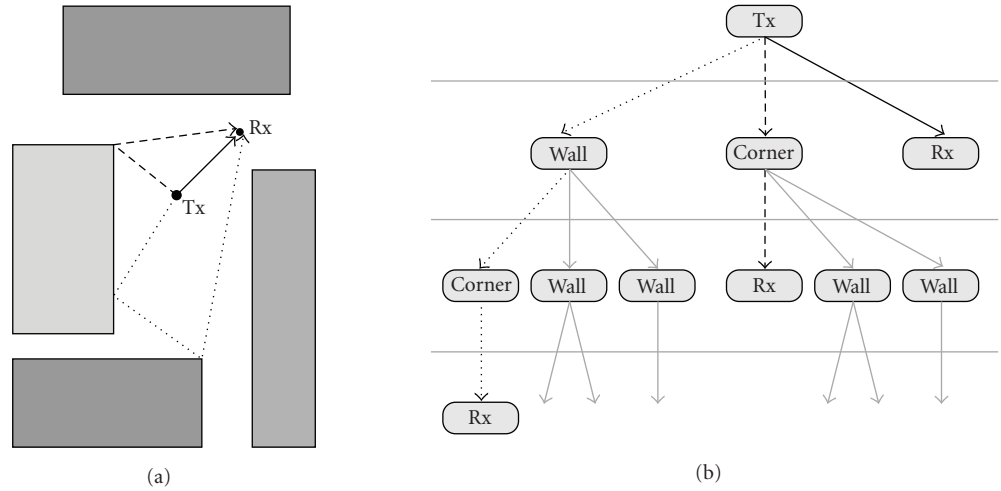

Figure 3: Simple RT illustration: (a) propagation scenario (gray shading indicates buildings); (b) corresponding visibility tree (first three layers shown).

the environment and of the radio link can be easily stored in files (environment databases) and the corresponding propagation process can be simulated through computer programs. Buildings are usually represented as polygonal prisms with flat tops, that is, they are composed of flat polygons (walls) and piecewise rectilinear edges. Deterministic models are physically meaningful, and potentially accurate. However, they are only representative for the environment considered. Hence, in many cases, multiple runs using different environments are required. Due to the high accuracy and adherence to the actual propagation process, deterministic models may be used to replace measurements when time is not sufficient to set up a measurement campaign or when particular cases, which are difficult to measure in the real world, will be studied. Although electromagnetic models such as the *method of moments* (MoM) or the *finite-difference in time domain* (FDTD) model may be useful to study near field problems in the vicinity of the Tx or Rx antennas, the most appropriate physical-deterministic models for radio propagation, at least in urban areas, are *ray tracing* (RT) models. RT models use the theory of geometrical optics to treat reflection and transmission on plane surfaces and diffraction on rectilinear edges [48]. Geometrical optics is based on the so-called ray approximation, which assumes that the wavelength is sufficiently small compared to the dimensions of the obstacles in the environment. This assumption is usually valid in urban radio propagation and allows to express the electromagnetic field in terms of a set of rays, each one of them corresponding to a piecewise linear path connecting two terminals. Each "corner" in a path corresponds to an "interaction" with an obstacle (e.g., wall reflection, edge diffraction). Rays have a null transverse dimension and therefore can in principle describe the field with infinite resolution. If beams (tubes of flux) with a finite transverse dimension are used instead of rays, then the resulting model is called *beam launching*, or ray splitting. Beam launching models allow faster field strength prediction but are less accurate in characterizing the radio channel between two SISO or MIMO terminals. Therefore, only RT models will be described in further detail here.

2.1.1. Ray-tracing algorithm

With RT algorithms, initially the Tx and Rx positions are specified and then all possible paths (rays) from the Tx to the Rx are determined according to geometric considerations and the rules of geometrical optics. Usually, a maximum number $N_{\max}$ of successive reflections/diffractions (often called prediction order) is prescribed. This geometric "ray tracing" core is by far the most critical and time consuming part of the RT procedure. In general, one adopts a strategy that captures the individual propagation paths via a so-called *visibility tree* (see Figure 3). The visibility tree consists of nodes and branches and has a layered structure. Each node of the tree represents an object of the scenario (a building wall, a wedge, the Rx antenna, dots) whereas each branch represents a line-of-sight (LoS) connection between two nodes/objects. The root node corresponds to the Tx antenna.

The visibility tree is constructed in a recursive manner, starting from the root of the tree (the Tx). The nodes in the first layer correspond to all objects for which there is an LoS to the Tx. In general, two nodes in subsequent layers are connected by a branch if there is LoS between the corresponding physical objects. This procedure is repeated until layer $N_{\max}$ (prediction order) is reached. Whenever the Rx is contained in a layer, the corresponding branch is terminated with a "leaf." The total number of leaves in the tree corresponds to the number of paths identified by the RT procedure. The

creation of the visibility tree may be highly computationally complex, especially in a full 3D case and if $N_{\max}$ is large.

Once the visibility tree is built, a backtracking procedure determines the path of each ray by starting from the corresponding leaf, traversing the tree upwards to the root node, and applying the appropriate geometrical optics rules at each traversed node. To the ith ray, a complex, vectorial electric field amplitude $\mathbf{E}_i$ is associated, which is computed by taking into account the Tx-emitted field, free space path loss, and the reflections, diffractions, and so forth experienced by the ray. Reflections are accounted for by applying the Fresnel reflection coefficients [48], whereas for diffractions the field vector is multiplied by appropriate diffraction coefficients obtained from the uniform geometrical theory of diffraction [49, 50]. The distance-decay law (divergence factor) may vary along the way due to diffractions (see [49]). The resulting field vector at the Rx position is composed of the fields for each of the N_r rays as $\mathbf{E}^{\mathrm{Rx}} = \sum_{i=0}^{N_r} \mathbf{E}_i^{\mathrm{Rx}}$ with

$$\mathbf{E}_i^{\mathrm{Rx}} = \Gamma_i \mathbf{B}_i \mathbf{E}_i^{\mathrm{Tx}} \quad \text{with } \mathbf{B}_i = \mathbf{A}_{i,N_i} \mathbf{A}_{i,N_i-1} \cdots \mathbf{A}_{i,1}. \tag{12}$$

Here, Γ_i is the overall divergence factor for the ith path (this depends on the length of all path segments and the type of interaction at each of its nodes), $\mathbf{A}_{i,j}$ is a rank-one matrix that decomposes the field into orthogonal components at the jth node (this includes appropriate attenuation, reflection, and diffraction coefficients and thus depends on the interaction type), $N_i \leq N_{\max}$ is the number of interactions (nodes) of the ith path, and $\mathbf{E}_i^{\mathrm{Tx}}$ is the field at a reference distance of 1 m from the Tx in the direction of the ith ray.

2.1.2. Application to MIMO channel characterization

To obtain the mapping of a channel input signal to the channel output signal (and thereby all elements of a MIMO channel matrix $\mathbf{H}$), (12) must be augmented by taking into account the antenna patterns and polarization vectors at the Tx and Rx [51]. Note that this has the advantage that different antenna types and configurations can be easily evaluated for the same propagation environment. Moreover, accurate, site-specific MIMO performance evaluation is possible (e.g., [52]).

Since all rays at the Rx are characterized individually in terms of their amplitude, phase, delay, angle of departure, and angle of arrival, RT allows a complete characterization of propagation [53] as far as specular reflections or diffractions are concerned. However, traditional RT methods neglect diffuse scattering which can be significant in many propagation environments (diffuse scattering refers to the power scattered in other than the specular directions which is due to nonideal scatterer surfaces). Since diffuse scattering increases the "viewing angle" at the corresponding node of the visibility tree, it effectively increases the number of rays. This in turn has a noticeable impact on temporal and angular dispersion and hence on MIMO performance. This fact has motivated growing recent interest in introducing some kind of diffuse scattering into RT models. For example, in [54], a simple diffuse scattering model has been inserted into a 3D RT method; RT augmented by diffuse scattering was seen to be in better agreement with measurements than classical RT without diffuse scattering.

2.2. Geometry-based stochastic physical models

Any geometry-based model is determined by the scatterer locations. In deterministic geometrical approaches (like RT discussed in the previous subsection), the scatterer locations are prescribed in a database. In contrast, geometry-based stochastic channel models (GSCM) choose the scatterer locations in a stochastic (random) fashion according to a certain probability distribution. The actual channel impulse response is then found by a simplified RT procedure.

2.2.1. Single-bounce scattering

GSCM were originally devised for channel simulation in systems with multiple antennas at the base station (diversity antennas, smart antennas). The predecessor of the GSCM in [55] placed scatterers in a deterministic way on a circle around the mobile station, and assumed that only single scattering occurs (i.e., one interacting object between Tx and Rx). Roughly twenty years later, several groups simultaneously suggested to augment this single-scattering model by using randomly placed scatterers [56–61]. This random placement reflects physical reality much better. The single-scattering assumption makes RT extremely simple: apart from the LoS, all paths consist of two subpaths connecting the scatterer to the Tx and Rx, respectively. These subpaths characterize the DoD, DoA, and propagation time (which in turn determines the overall attenuation, usually according to a power law). The scatterer interaction itself can be taken into account via an additional random phase shift.

A GSCM has a number of important advantages [62]:

(i) it has an immediate relation to physical reality; important parameters (like scatterer locations) can often be determined via simple geometrical considerations;
(ii) many effects are implicitly reproduced: small-scale fading is created by the superposition of waves from individual scatterers; DoA and delay drifts caused by MS movement are implicitly included;
(iii) all information is inherent to the distribution of the scatterers; therefore, dependencies of power delay profile (PDP) and angular power spectrum (APS) do not lead to a complication of the model;
(iv) Tx/Rx and scatterer movement as well as shadowing and the (dis)appearance of propagation paths (e.g., due to blocking by obstacles) can be easily implemented; this allows to include long-term channel correlations in a straightforward way.

Different versions of the GSCM differ mainly in the proposed scatterer distributions. The simplest GSCM is obtained by assuming that the scatterers are spatially uniformly distributed. Contributions from far scatterers carry less power since they propagate over longer distances and are thus attenuated more strongly; this model is also often called single-bounce geometrical model. An alternative approach

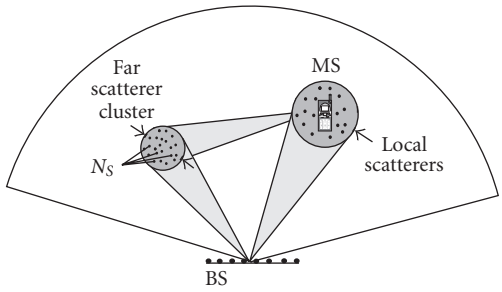

Figure 4: Principle of the GSCM (BS—base station, MS—mobile station).

suggests to place the scatterers randomly around the MS [58, 60]. In [63], various other scatterer distributions around the MS were analyzed; a one-sided Gaussian distribution with respect to distance from the MS resulted in an approximately exponential PDP, which is in good agreement with many measurement results. To make the density or strength of the scatterers depend on distance, two implementations are possible. In the "classical" approach, the probability density function of the scatterers is adjusted such that scatterers occur less likely at large distances from the MS. Alternatively, the "nonuniform scattering cross section" method places scatterers with uniform density in the considered area, but down-weights their contributions with increasing distance from the MS [62]. For very high scatterer density, the two approaches are equivalent. However, nonuniform scattering cross-section can have numerical advantages, in particular less statistical fluctuations of the power-delay profile when the number of scatterers is finite.

Another important propagation effect arises from the existence of clusters of far scatterers (e.g., large buildings, mountains, and so forth). Far scatterers lead to increased temporal and angular dispersion and can thus significantly influence the performance of MIMO systems. In a GSCM, they can be accounted for by placing clusters of far scatterers at random locations in the cell [60] (see Figure 4).

2.2.2. Multiple-bounce scattering

All of the above considerations are based on the assumption that only single-bounce scattering is present. This is restrictive insofar as the position of a scatterer completely determines DoD, DoA, and delay, that is, only two of these parameters can be chosen independently. However, many environments (e.g., micro- and picocells) feature multiple-bounce scattering for which DoD, DoA, and delay are completely decoupled. In microcells, the BS is below rooftop height, so that propagation mostly consists of waveguiding through street canyons [64, 65], which involves multiple reflections and diffractions (this effect can be significant even in macrocells [66]). For picocells, propagation within a single large room is mainly determined by LoS propagation and single-bounce reflections. However, if the Tx and Rx are in different rooms, then the radio waves either propagate through the walls or they leave the Tx room, for example, through a window or door, are waveguided through a corridor, and be diffracted into the room with the Rx [67].

If the directional channel properties need to be reproduced only for *one* link end (i.e., multiple antennas only at the Tx or Rx), multiple-bounce scattering can be incorporated into a GSCM via the concept of *equivalent scatterers*. These are virtual single-bounce scatterers whose positions and pathloss are chosen such that they mimic multiple bounce contributions in terms of their delay and DoA (see Figure 5). This is always possible since the delay, azimuth, and elevation of a single-bounce scatterer are in one-to-one correspondence with its Cartesian coordinates. A similar relationship exists on the level of statistical characterizations for the joint angle-delay power spectrum and the probability density function of the scatterer coordinates (i.e., the spatial scatterer distribution). For further details, we refer to [17].

In a MIMO system, the equivalent scatterer concept fails since the angular channel characteristics are reproduced correctly only for one link end. As a remedy, [68] suggested the use of double scattering where the coupling between the scatterers around the BS and those around the MS is established by means of a so-called illumination function (essentially a DoD spectrum relative to that scatterer). We note that the channel model in that paper also features simple mechanisms to include waveguiding and diffraction.

Another approach to incorporate multiple-bounce scattering into GSCM models is the twin-cluster concept pursued within COST 273 [11]. Here, the BS and MS views of the scatterer positions are different, and a coupling is established in terms of a stochastic link delay. This concept indeed allows for decoupled DoA, DoD, and delay statistics.

2.3. Nongeometrical stochastic physical models

Nongeometrical stochastic models describe paths from Tx to Rx by statistical parameters only, without reference to the geometry of a physical environment. There are two classes of stochastic nongeometrical models reported in the literature. The first one uses clusters of MPCs and is generally called the extended Saleh-Valenzuela model since it generalizes the temporal cluster model developed in [69]. The second one (known as Zwick model) treats MPCs individually.

2.3.1. Extended Saleh-Valenzuela model

Saleh and Valenzuela proposed to model clusters of MPCs in the delay domain via a doubly exponential decay process [69] (a previously considered approach used a two-state Poisson process [65]). The Saleh-Valenzuela model uses one exponentially decaying profile to control the power of a multipath cluster. The MPCs within the individual clusters are then characterized by a second exponential profile with a steeper slope.

The Saleh-Valenzuela model has been extended to the spatial domain in [21, 70]. In particular, the extended Saleh-Valenzuela MIMO model in [21] is based on the assumptions that the DoD and DoA statistics are independent and identical. (This is unlikely to be exactly true in practice; however,

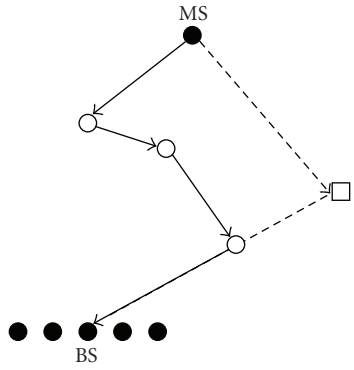

Figure 5: Example for equivalent scatterer (□) in the uplink of a system with multiple element BS antenna (true scatterers shown as ○).

no contrary evidence was initially available since the model was developed from SIMO measurements.) These assumptions allow to characterize the spatial clusters in terms of their mean cluster angle and the cluster angular spread (cf. [71]). Usually, the mean cluster angle Θ is assumed to be uniformly distributed within $[0, 2\pi)$ and the angle φ of the MPCs in the cluster are Laplacian distributed, that is, their probability density function equals

$$p(\varphi) = \frac{c}{\sqrt{2}\sigma} \exp\left(- \frac{\sqrt{2}}{\sigma} |\varphi - \Theta| \right), \tag{13}$$

where σ characterizes the cluster's angular spread and c is an appropriate normalization constant [35]. The mean delay for each cluster is characterized by a Poisson process, and the individual delays of the MPCs within the cluster are characterized by a second Poisson process relative to the mean delay.

2.3.2. Zwick model

In [72] it is argued that for indoor channels clustering and multipath fading do not occur when the sampling rate is sufficiently large. Thus, in the Zwick model, MPCs are generated independently (no clustering) and without amplitude fading. However, phase changes of MPCs are incorporated into the model via geometric considerations describing Tx, Rx, and scatterer motion. The geometry of the scenario of course also determines the existence of a specific MPC, which thus appears and disappears as the channel impulse response evolves with time. For nonline of sight (NLoS) MPCs, this effect is modeled using a marked Poisson process. If a line-of-sight (LoS) component will be included, it is simply added in a separate step. This allows to use the same basic procedure for both LoS and NLoS environments.

3. ANALYTICAL MODELS

3.1. Correlation-based analytical models

Various narrowband analytical models are based on a *multivariate complex Gaussian distribution* [21] of the MIMO channel coefficients (i.e., Rayleigh or Ricean fading). The channel matrix can be split into a zero-mean stochastic part $\mathbf{H}_s$ and a purely deterministic part $\mathbf{H}_d$ according to (e.g., [73])

$$\mathbf{H} = \sqrt{\frac{1}{1+K}}\mathbf{H}_s + \sqrt{\frac{K}{1+K}}\mathbf{H}_d, \tag{14}$$

where $K \geq 0$ denotes the Rice factor. The matrix $\mathbf{H}_d$ accounts for LoS components and other nonfading contributions. In the following, we focus on the NLoS components characterized by the Gaussian matrix $\mathbf{H}_s$. For simplicity, we thus assume $K = 0$, that is, $\mathbf{H} = \mathbf{H}_s$. In its most general form, the zero-mean multivariate complex Gaussian distribution of $\mathbf{h} = \text{vec}\{\mathbf{H}\}$ is given by[7]

$$f(\mathbf{h}) = \frac{1}{\pi^{nm}\det\{\mathbf{R}_\mathbf{H}\}} \exp\left(- \mathbf{h}^H \mathbf{R}_\mathbf{H}^{-1} \mathbf{h} \right). \tag{15}$$

The $nm \times nm$ matrix

$$\mathbf{R}_\mathbf{H} = E\{\mathbf{h}\mathbf{h}^H\} \tag{16}$$

is known as *full correlation matrix* (e.g., [27, 28]) and describes the spatial MIMO channel statistics. It contains the correlations of all channel matrix elements. Realizations of MIMO channels with distribution (15) can be obtained by[8]

$$\mathbf{H} = \text{unvec}\{\mathbf{h}\} \quad \text{with } \mathbf{h} = \mathbf{R}_\mathbf{H}^{1/2}\mathbf{g}. \tag{17}$$

Here, $\mathbf{R}_\mathbf{H}^{1/2}$ denotes an arbitrary matrix square root (i.e., any matrix satisfying $\mathbf{R}_\mathbf{H}^{1/2}\mathbf{R}_\mathbf{H}^{H/2} = \mathbf{R}_\mathbf{H}$), and $\mathbf{g}$ is an $nm \times 1$ vector with i.i.d. Gaussian elements with zero mean and unit variance.

Note that direct use of (17) in general requires full specification of $\mathbf{R}_\mathbf{H}$ which involves $(nm)^2$ real-valued parameters. To reduce this large number of parameters, several different models were proposed that impose a particular structure on the MIMO correlation matrix. Some of these models will next be briefly reviewed. For further details, we refer to [74].

3.1.1. The i.i.d. model

The simplest analytical MIMO model is the i.i.d. model (sometimes referred to as canonical model). Here $\mathbf{R}_\mathbf{H} = \rho^2\mathbf{I}$, that is, all elements of the MIMO channel matrix $\mathbf{H}$ are uncorrelated (and hence statistically independent) and have equal variance ρ^2. Physically, this corresponds to a spatially white MIMO channel which occurs only in rich scattering environments characterized by independent MPCs uniformly distributed in all directions. The i.i.d. model consists just of a single parameter (the channel power ρ^2) and is often used for theoretical considerations like the information theoretic analysis of MIMO systems [1].

[7] For an $n \times m$ matrix $\mathbf{H} = [\mathbf{h}_1 \cdots \mathbf{h}_m]$, the vec$\{\cdot\}$ operator returns the length-nm vector $\text{vec}\{\mathbf{H}\} = [\mathbf{h}_1^T \cdots \mathbf{h}_m^T]^T$.

[8] Here, unvec$\{\cdot\}$ is the inverse operator of vec$\{\cdot\}$.

3.1.2. The Kronecker model

The so-called Kronecker model was used in [25–27] for capacity analysis before being proposed by [28] in the framework of the European Union SATURN project [75]. It assumes that spatial Tx and Rx correlation are separable, which is equivalent to restricting to correlation matrices that can be written as Kronecker product

$$\mathbf{R}_{\mathbf{H}} = \mathbf{R}_{\mathrm{Tx}} \otimes \mathbf{R}_{\mathrm{Rx}} \tag{18}$$

with the Tx and Rx correlation matrices

$$\mathbf{R}_{\mathrm{Tx}} = E\{\mathbf{H}^H\mathbf{H}\}, \qquad \mathbf{R}_{\mathrm{Rx}} = E\{\mathbf{H}\mathbf{H}^H\}, \tag{19}$$

respectively. It can be shown that under the above assumption, (17) simplifies to the *Kronecker model*

$$\mathbf{h} = \left(\mathbf{R}_{\mathrm{Tx}} \otimes \mathbf{R}_{\mathrm{Rx}}\right)^{1/2}\mathbf{g} \Longleftrightarrow \mathbf{H} = \mathbf{R}_{\mathrm{Rx}}^{1/2}\mathbf{G}\mathbf{R}_{\mathrm{Tx}}^{1/2} \tag{20}$$

with $\mathbf{G} = \mathrm{unvec}(\mathbf{g})$ an i.i.d. unit-variance MIMO channel matrix. The model requires specification of the Tx and Rx correlation matrices, which amounts to $n^2 + m^2$ real parameters (instead of n^2m^2).

The main restriction of the Kronecker model is that it enforces a separable DoD-DoA spectrum [76], that is, the joint DoD-DoA spectrum is the product of the DoD spectrum and the DoA spectrum. Note that the Kronecker model is not able to reproduce the coupling of a single DoD with a single DoA, which is an elementary feature of MIMO channels with single-bounce scattering.

Nonetheless, the model (20) has been used for the theoretical analysis of MIMO systems and for MIMO channel simulation yielding experimentally verified results when two or maximum three antennas at each link end were involved. Furthermore, the underlying separability of Tx and Rx in the Kronecker sense allows for independent array optimization at Tx and Rx. These applications and its simplicity have made the Kronecker model quite popular.

3.1.3. The Weichselberger model

The Weichselberger model [29, 74] aims at obviating the restriction of the Kronecker model to separable DoA-DoD spectra that neglects significant parts of the spatial structure of MIMO channels. Its definition is based on the eigenvalue decomposition of the Tx and Rx correlation matrices,

$$\begin{aligned}\mathbf{R}_{\mathrm{Tx}} &= \mathbf{U}_{\mathrm{Tx}}\mathbf{\Lambda}_{\mathrm{Tx}}\mathbf{U}_{\mathrm{Tx}}^H,\\ \mathbf{R}_{\mathrm{Rx}} &= \mathbf{U}_{\mathrm{Rx}}\mathbf{\Lambda}_{\mathrm{Rx}}\mathbf{U}_{\mathrm{Rx}}^H.\end{aligned} \tag{21}$$

Here, $\mathbf{U}_{\mathrm{Tx}}$ and $\mathbf{U}_{\mathrm{Rx}}$ are unitary matrices whose columns are the eigenvectors of $\mathbf{R}_{\mathrm{Tx}}$ and $\mathbf{R}_{\mathrm{Rx}}$, respectively, and $\mathbf{\Lambda}_{\mathrm{Tx}}$ and $\mathbf{\Lambda}_{\mathrm{Rx}}$ are diagonal matrices with the corresponding eigenvalues. The model itself is given by

$$\mathbf{H} = \mathbf{U}_{\mathrm{Rx}}(\widetilde{\mathbf{\Omega}} \odot \mathbf{G})\mathbf{U}_{\mathrm{Tx}}^T, \tag{22}$$

where $\mathbf{G}$ is again an $n \times m$ i.i.d. MIMO matrix, $\odot$ denotes the Schur-Hadamard product (elementwise multiplication), and

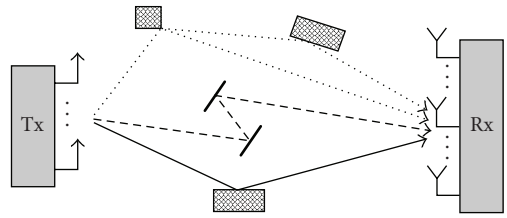

Figure 6: Example of finite scatterer model with single-bounce scattering (solid line), multiple-bounce scattering (dashed line), and a "split" component (dotted line).

$\widetilde{\mathbf{\Omega}}$ is the elementwise square root of an $n \times m$ coupling matrix $\mathbf{\Omega}$ whose (real-valued and nonnegative) elements determine the average power coupling between the Tx and Rx eigenmodes. This coupling matrix allows for *joint* modeling of the Tx and Rx channel correlations. We note that the Kronecker model is a special case of the Weichselberger model obtained with the *rank-one* coupling matrix $\mathbf{\Omega} = \boldsymbol{\lambda}_{\mathrm{Rx}}\boldsymbol{\lambda}_{\mathrm{Tx}}^T$, where $\boldsymbol{\lambda}_{\mathrm{Tx}}$ and $\boldsymbol{\lambda}_{\mathrm{Rx}}$ are vectors containing the eigenvalues of the Tx and Rx correlation matrix, respectively.

The Weichselberger model requires specification of the Tx and Rx eigenmodes ($\mathbf{U}_{\mathrm{Tx}}$ and $\mathbf{U}_{\mathrm{Rx}}$) and of the coupling matrix $\mathbf{\Omega}$. In general, this amounts to $n(n-1)+m(m-1)+nm$ real parameters. These are directly obtainable from measurements. We emphasize, however, that capacity (mutual information) and diversity order of a MIMO channel are independent of the Tx and Rx eigenmodes; hence, their analysis requires only the coupling matrix $\mathbf{\Omega}$ (nm parameters). In particular, the structure of $\mathbf{\Omega}$ determines which MIMO gains (diversity, capacity, or beamforming gain) can be exploited which helps to design signal-processing algorithms. Some instructive examples are discussed in [74, Chapter 6.4.3.4].

3.2. Propagation-motivated analytical models

3.2.1. Finite scatterer model

The fundamental assumption of the finite scatterer model is that propagation can be modeled in terms of a finite number P of multipath components (cf. Figure 6). For each of the components (indexed by p), a DoD ϕ_p, DoA ψ_p, complex amplitude ξ_p, and delay τ_p is specified.[9]

The model allows for single-bounce and multiple-bounce scattering, which is in contrast to GSCMs that usually only incorporate single-bounce and double-bounce scattering. The finite scatterer models even allow for "split" components (see Figure 6), which have a single DoD but subsequently split into two or more paths with different DoAs (or vice versa). The split components can be treated as multiple components having the same DoD (or DoA). For more details we refer to [22, 77].

[9] For simplicity, we restrict to the 2D case where DoA and DoD are characterized by their azimuth angles. All of the subsequent discussion is easily generalized to the 3D case by including the elevation angle into DoA and DoD.

Given the parameters of all MPCs, the MIMO channel matrix $\mathbf{H}$ for the narrowband case (i.e., neglecting the delays τ_p) is given by

$$\mathbf{H} = \sum_{p=1}^{P} \xi_p \boldsymbol{\psi}(\psi_p)\boldsymbol{\phi}^T(\phi_p) = \boldsymbol{\Psi}\boldsymbol{\Xi}\boldsymbol{\Phi}^T, \tag{23}$$

where $\boldsymbol{\Phi} = [\boldsymbol{\phi}(\phi_1)\cdots\boldsymbol{\phi}(\phi_P)]$, $\boldsymbol{\Psi} = [\boldsymbol{\psi}(\psi_1)\cdots\boldsymbol{\psi}(\psi_P)]$, $\boldsymbol{\phi}^T(\phi_p)$ and $\boldsymbol{\psi}(\psi_p)$ are the Tx and Rx steering vectors corresponding to the pth MPC, and $\boldsymbol{\Xi} = \mathrm{diag}(\xi_1,\ldots,\xi_P)$ is a diagonal matrix consisting of the multipath amplitudes. Note that the steering vectors incorporate the geometry, directivity, and coupling of the antenna array elements. For wideband systems, also the delays must be taken into account. Including the bandlimitation to the system bandwidth $B = 1/T_s$ into the channel, the resulting tapped delay line representation of the channel reads $\mathbf{H}(\tau) = \sum_{l=-\infty}^{\infty} \mathbf{H}_l \delta(\tau - lT_s)$ with

$$\mathbf{H}_l = \sum_{p=1}^{P} \xi_p \mathrm{sinc}(\tau_p - lT_s)\boldsymbol{\psi}(\psi_p)\boldsymbol{\phi}^T(\phi_p) = \boldsymbol{\Psi}(\boldsymbol{\Xi}\odot\mathbf{T}_l)\boldsymbol{\Phi}^T, \tag{24}$$

where $\mathrm{sinc}(x) = \sin(\pi x)/(\pi x)$ and $\mathbf{T}_l$ is a diagonal matrix with diagonal elements $\mathrm{sinc}(\tau_p - lT_s)$, $p = 1,\ldots,P$. Further details can be found in [78].

The finite scatterer model can be interpreted as a straightforward way to calculate (10) (see Section 1.3.3). It is compatible with many other models (e.g., the 3GPP model [30]) that define statistical distributions for the MPC parameters. Other environment dependent distributions of these parameters may be inferred from measurements. For example, the measurements in [78] suggest that in an urban environment all multipath parameters are statistically independent and the DoAs ψ_p and DoDs ϕ_p are approximately uniformly distributed, the complex amplitudes ξ_p have a log-normally distributed magnitude and uniform phase, and the delays τ_p are exponentially distributed.

3.2.2. Maximum entropy model

In [23], the question of MIMO channel modeling based on statistical inference was addressed. In particular, the maximum entropy principle was proposed to determine the distribution of the MIMO channel matrix based on a priori information that is available. This a priori information might include properties of the propagation environment and system parameters (e.g., bandwidth, DoAs, etc.). The maximum entropy principle was justified by the objective to avoid any model assumptions not supported by the prior information. As far as consistency is concerned, [23] shows that the target application for which the model has to be consistent can influence the proper choice of the model. Hence, one may obtain different channels models for capacity calculations than for bit-error-rate simulations. Since this is obviously undesirable, it was proposed to ignore information about any target application when constructing practically useful models. Consistency is then enforced by the following axiom.

Axiom

If the prior information $\mathbf{I_1}$ which is the basis for channel model $\mathbf{H_1}$ is equivalent to the prior information $\mathbf{I_2}$ of channel model $\mathbf{H_2}$, then both models must be assigned the same probability distribution, $f(\mathbf{H_1}) = f(\mathbf{H_2})$.

As an example, consider that the following prior information is available:

(i) the numbers s_{Tx} and s_{Rx} of scatterers at the Tx and Rx side, respectively;
(ii) the steering vectors for all Tx and Rx scatterers, contained in the $m \times s_{\mathrm{Tx}}$ and $n \times s_{\mathrm{Rx}}$ matrices $\boldsymbol{\Phi}$ and $\boldsymbol{\Psi}$, respectively;
(iii) the corresponding scatterer powers $\mathbf{P}_{\mathrm{Tx}}$ and $\mathbf{P}_{\mathrm{Rx}}$; and
(iv) the path gains between Tx and Rx scatterers, characterized by $s_{\mathrm{Rx}} \times s_{\mathrm{Tx}}$ pattern mask (coupling matrix) $\boldsymbol{\Omega}$.

Then, the maximum entropy channel model was shown to equal

$$\mathbf{H} = \boldsymbol{\Psi}\mathbf{P}_{\mathrm{Rx}}^{1/2}(\boldsymbol{\Omega}\odot\mathbf{G})\mathbf{P}_{\mathrm{Tx}}^{1/2}\boldsymbol{\Phi}^T, \tag{25}$$

where $\mathbf{G}$ is an $s_{\mathrm{Rx}} \times s_{\mathrm{Tx}}$ Gaussian matrix with i.i.d. elements. We note that this model is consistent in the sense that less detailed models (for which parts of the prior information are not available) can be obtained by "marginalizing" (25) with respect to the unknown parameters.[10] Examples include the i.i.d. Gaussian model where only the channel energy is known (obtained with $\boldsymbol{\Phi} = \mathbf{F}_m$ where $\mathbf{F}_m$ is the length-m DFT matrix, $\boldsymbol{\Psi} = \mathbf{F}_n$, $\mathbf{P}_{\mathrm{Tx}} = \mathbf{I}$, and $\mathbf{P}_{\mathrm{Rx}} = \mathbf{I}$), the DoA model where steering vectors and powers are known only for the Rx side (obtained with $\boldsymbol{\Phi} = \mathbf{F}_m$, $\mathbf{P}_{\mathrm{Tx}} = \mathbf{I}$), and the DoD model where steering vectors and powers are known only for the Tx side (obtained with $\boldsymbol{\Psi} = \mathbf{F}_n$, $\mathbf{P}_{\mathrm{Rx}} = \mathbf{I}$). We conclude that a useful feature of the maximum entropy approach is the simplicity of translating an increase or decrease of (physical) prior information into the channel distribution model in a consistent fashion.

3.2.3. Virtual channel representation

In [24], a MIMO model called virtual channel representation was proposed as follows:

$$\mathbf{H} = \mathbf{F}_n(\boldsymbol{\Omega}\odot\mathbf{G})\mathbf{F}_m^H. \tag{26}$$

Here, the DFT matrices $\mathbf{F}_m$ and $\mathbf{F}_n$ contain the steering vectors for m virtual Tx and n virtual Rx scatterers, $\mathbf{G}$ is an $n \times m$ i.i.d. zero-mean Gaussian matrix, and $\boldsymbol{\Omega}$ is an $n \times m$ matrix whose elements characterize the coupling of each pair of virtual scatterers, that is, $(\boldsymbol{\Omega}\odot\mathbf{G})$ represents the "inner" propagation environment between virtual Tx and Rx scatterers. In essence, (26) corresponds to a spatial sampling that collapses all physical DoAs and DoDs into fixed directions

[10] Models that do not have this property can be shown to contradict Bayes' law.

determined by the spatial resolution of the arrays. We note that the virtual channel model can be viewed as a special case of the Weichselberger model with Tx and Rx eigenmodes equal to the columns of the DFT matrices. In the case where $[\mathbf{\Omega}]_{ij} = 1$, the virtual channel model reduces to the i.i.d. channel model, that is, rich scattering with full connection of (virtual) Tx and Rx scatterer clusters. Due to its simplicity, the virtual channel model is mostly useful for theoretical considerations like analyzing the capacity scaling behavior of MIMO channels [79]. It was also shown to be capacity complying in [80, 81]. However, one has to keep in mind that the virtual representation in terms of DFT steering matrices is appropriate only for uniform linear arrays at Tx and Rx.

4. STANDARDIZED MODELS

Standardized models are an important tool for the development of new radio systems. They allow to assess the benefits of different techniques (signal processing, multiple access, etc.) for enhancing capacity and improving performance, in a manner that is unified and agreed on by many parties. For example, the COST 207 wideband power delay profile model was widely used in the development of GSM, and used as a basis for the decision on modulation and multiple-access methods. In this section, we discuss five standardized directional MIMO channel models to provide an overview of recent and ongoing channel modeling activities.

4.1. COST 259/273

"COST" is an abbreviation for *European cooperation in the field of scientific and technical research*. Several COST initiatives were dedicated to wireless communications, in particular COST 259 "Flexible personalized wireless communications" (1996–2000) and COST 273 "Towards mobile broadband multimedia networks" (2001–2005). These initiatives developed channel models that include directional characteristics of radio propagation and are thus suitable for the simulation of smart antennas and MIMO systems. They are, at this time, the most general standardized channel models, and are not intended for specific systems. The 3GPP/3GPP2 model and the 802.11n model can be viewed as subsets (though with different parameter settings).

4.1.1. COST 259 directional channel model

The COST 259 directional channel model (DCM) [17, 18] is a physical model that gives a model for the delay and angle dispersion at BS and MS, for different radio environments. It was the first model that explicitly took the rather complex relationships between BS-MS-distance, delay dispersion, angular spread, and other parameters into account. It is also general in the sense that it is defined for a 13 different radio environments (e.g., typical urban, bad urban, open square, indoor office, indoor corridor) that include macrocellular, microcellular, and picocellular scenarios.[11] The modeling approaches for macro-, micro-, and picocells are different; in the following, we describe only the macrocell approach.

Each radio environment is described by *external* parameters (e.g., BS position, radio frequency, average BS and MS height) and by *global* parameters, which are sets of probability density functions and/or statistical moments characterizing a specific environment (e.g., the number of scatterers is characterized by a Poisson distribution). The determination of the global parameters is partly geometric, and partly stochastic. We place the MS at random in the cell. Similarly, a number of scatterer clusters (see Section 2.2.1) are geometrically placed in the cell. From those positions, we can determine the relative delay and mean angles of the different clusters that make up the double-directional impulse response. The angular spread, delay spread, and shadowing, on the other hand, are determined stochastically. They are modeled as correlated lognormally distributed random variables.

Each *radio environment* contains a number of *propagation environments*, which are defined as an area over which the local parameters (which are defined as realizations of the global parameters) are approximately constant; they are typically several meters in diameter. These local parameters are randomly generated realizations of the global parameters and describe the instantaneous channel behavior. As ultimate output of the channel model, the double-directional impulse response is then obtained according to (1)-(2), which then allows to derive the transfer function matrix according to (10). The impulse responses can also be generated via a GSCM approach, as described in Section 2.2. It is noteworthy that the COST 259 model can handle the continuous movement of the MS over several propagation environments, and even across different radio environments; details can be found in [17, 18].

While fairly general, there are two major restrictions of the COST 259 DCM. On the one hand, scatterers are assumed *stationary* so that channel time variations are solely due to MS movement; this obviously excludes certain environments (e.g., indoor scenarios with persons moving around). On the other hand, delay attenuations are modeled as complex Gaussian random variables. This requires a sufficiently large number of MPCs within each delay bin, a condition that is not met in some situations; this latter assumption is also made in all other standardized channel models.

4.1.2. COST 273

The COST 273 channel model [82] shows considerable similarity to the COST 259 model, but differs in several key respects.

[11] *Macrocells* have outdoor BSs above rooftop and either outdoor MSs at street level or indoor MSs. The BS and MS environments are thus quite different. Cell sizes are typically in the kilometer range. *Microcells* differ from macrocells by having outdoor BSs *below* rooftop. The BS and MS environments here are thus more similar than in macrocells. *Picocells* have indoor BSs and much smaller cell size.

(1) A number of new radio environments is defined, reflecting the new applications for MIMO systems (e.g., peer-to-peer and fixed-wireless-access scenarios).

(2) The chosen parameters have been updated, based on new available measurement campaigns.

(3) The same modeling approach is used for macro-, micro-, and pico-cells. The approach is similar to the COST 259 approach for macrocells.

(4) The modeling of the distribution of DOAs and DODs is different, compared to the COST 259 model. One cluster is split up into two representations of itself: one that represents the cluster as seen by the BS and one as it is seen by the mobile terminal (MT). Both realizations look identical, like twins. Each ray propagated at the transmitter is bounced at each scatterer in the corresponding cluster and reradiated at the same scatterer of the twin cluster towards the receiver. The two cluster representations are linked via a *stochastic cluster link delay*, which is the same for all scatterers inside a cluster. The cluster link delay ensures realistic path delays as, for example, derived from measurement campaigns, whereas the placement of the cluster is driven by the angular statistics of the cluster as observed from BS/MT, respectively.

4.2. 3GPP SCM

The spatial channel model (SCM) [30] was developed by 3GPP/3GPP2 to be a common reference for evaluating different MIMO concepts in outdoor environments at a center frequency of 2 GHz and a system bandwidth of 5 MHz.

The SCM consists of two parts: (i) a calibration model, and (ii) a system-simulation model.

4.2.1. Calibration model

The calibration model is an over-simplified channel model whose purpose is to check the correctness of simulation implementations. In the course of standardization work, it is often necessary to compare the implementations of the *same algorithm by different companies*. Comparing the performance of the algorithm in the "calibration" channels allows to easily assess whether two implementations are equivalent. We stress that the calibration model is *not* intended for performance assessment of algorithms or systems.

The calibration model, as described in the 3GPP/3GPP2 standard, can be implemented either as a physical model or as an analytical model. The physical model is a non-geometrical stochastic physical model (compare Section 2.3). It is a spatial extension of the ITU-R channel models [83], which describe the wideband characteristics of the channel as a tapped delay line. Taps with different delays are independently fading, and each tap is characterized by its own power azimuth spectrum (which is uniform or Laplacian), angular spread (AS), and mean direction, at both the MS and the BS. The parameters (i.e., angular spread, mean direction, etc.), are fixed; thus the model represents stationary channel conditions. The Doppler spectrum is defined implicitly by introducing speed and direction of travel of the MS.

The model also defines a number of antenna configurations. Given those, the physical model can be transformed into an equivalent analytical model as discussed in Section 3.2.1.

4.2.2. Simulation model

The SCM intended for performance evaluation is called the simulation model.[12] The model is a physical model and distinguishes between three different environments: urban macrocell, suburban macrocell, and urban microcell. The model structure and simulation methodology are identical for all these environments, but the parameters, like angular spread, delay spread, and so forth, are different.

The simulation model employs both geometrical and stochastic components. Let us first describe the simulation procedure for a single link between one MS and one BS. The geometrical component is that the MSs are placed at random within a given cell, and the orientation of the antenna array, as well as the direction of movement within the cell, are also chosen at random. From the MS position, we can determine the bulk pathloss, which is given by the COST 231—Hata model for macrocells, and the COST 231—Walfish-Ikegami model for microcells. The number of taps with different delays is 6 (as in the ITU-R models), but their delay and average power are chosen stochastically from a probability density function.

Each tap shows angular dispersion at the BS and the MS; this dispersion is implemented by representing each tap by a number of subpaths that all have the same delay, but different DOAs (and DODs). Physically, this means that each path consists of a cluster of 20 scatterers with slightly different directions but equal time of arrival. Specifically, the modeling of the angular dispersion works as follows: the mean DOA and DOD of the total arriving power (weighted average over all the taps) is determined by the location of the MS and the orientation of the antenna array. The mean DOA (or DOD) of one tap is chosen at random from a Gaussian distribution that is centered around this total mean (the variance of this distribution is one of the model parameters). The 20 subpaths have different offsets $\Delta\phi_i$ from this tap mean; those offsets are fixed and tabulated in the 3GPP standard. Adding up the different subpaths (which all have deterministic amplitudes, but different phases) results in Rayleigh or Rice fading. Temporal variations of the impulse response are effected by movement of the MS, which in turn leads to different phase shifts of the subpaths.

When using the SCM, the simulation of the system behavior is carried out as a sequence of "drops," where a "drop" is defined as one simulation run over a certain (short) time period. That period is assumed to be short, so that it is justified to assume (as the model does) that large-scale channel parameters, such as angle spread, mean DOA, delay spread, and shadowing stay constant during a drop. For each drop, these large-scale channel parameters are drawn according to

[12] This name, which is historically motivated, is slightly misleading, as the model is also intended for the performance evaluation of a single link.

distributions functions. The MS positions are varied at random at the beginning of each drop.

In some cases, we wish to emulate the channels between *multiple BS* cells/sectors and *multiple MSs* linked to these BSs. The cell layout and BS locations are fixed for a certain number of successive drops, but (as in the single-cell case) the MS positions are varied at random at the beginning of each drop.

Antenna radiation patterns, antenna geometries, and orientations can be chosen arbitrary, that is, the model is antenna independent. When all the parameters and antenna effects are defined, analytical formulations can be extracted from the physical model. Note that each drop results in a different correlation matrix for the analytical model.

In addition to the characteristics described above, the simulation model has several optional features: (i) a polarization model, (ii) far scatterer clusters, (iii) a LoS component for the microcellular case, and (iv) a modified distribution of the angular distribution at the MS, which emulates propagation in an urban street canyon.

4.3. WINNER channel models

The channel models developed in the IST-WINNER [31] project are related to both the COST 259 model (see Section 4.1.1) and the 3GPP SCM model (see Section 4.2). The WINNER models adopted the GSCM principle, the drop concept, and the generic approach to model all scenarios with the same generic structure. Generic multilink models are intended for system-level simulations, while clustered delay line (CDL) models, with fixed small scale parameters, are used for calibration simulations. Various measurement campaigns provide the background for the parameterization of seven indoor, urban, suburban and rural scenarios for both LOS and NLOS conditions. These measurements were conducted by five partners with different devices in different European countries.

In the first stage of the WINNER modeling work, the 3GPP SCM model was selected for immediate simulation needs. Due to the narrow bandwidth and the limited frequency applicability range, the SCM model was extended to the SCM-Extended (SCME) model [84] in following ways. The bandwidth was extended to 100 MHz by introducing the so-called intracluster delay spread. Center frequencies of 5 GHz were included by defining corresponding path-loss functions. Further upgrades to the original model include the LOS option for all three SCM scenarios, tapped-delay-line models and time evolution of small scale parameters together with evolution of shadow fading. A MATLAB implementation of the SCME is available on [31]. A reduced version of this model was adopted for standardization of the 3GPP long term evolution (LTE).

Another extension resulted in the WINNER Phase I channel model, which is reported in [31, deliverable D5.4] and [85]. It was developed to fill the shortage of measurement-based wideband system-level models for a wide set of scenarios. The novel features of the model are its parameterization, the consideration of elevation in indoor scenarios, autocorrelation modeling of large-scale parameters (including cross-correlation), and scenario-dependent polarization modeling. The model is scalable from a single SISO or MIMO link to a multilink MIMO scenario including polarization among other radio channel dimensions. A MATLAB implementation of this model is also available on [31].

4.4. IEEE 802.11n

The TGn channel model [33] of IEEE 802.11 was developed for indoor environments in the 2 GHz and 5 GHz bands, with a focus on MIMO WLANs. Measurement results from these two frequency bands were combined to develop the models (in fact, only the pathloss model depends on the frequency band). Environments like small and large offices, residential homes, and open spaces are considered, both with LoS and NLoS. The TGn channel model specifies a set of six environments (A to F), which mostly correspond to the single antenna WLAN channel models presented in [86, 87]. For each of the six environments, the TGn model specifies corresponding parameter sets. An implementation is available at [88].

The 802.11 TGn model is a physical model, using a nongeometric stochastic approach, somewhat similar to the 3GPP/3GPP2 model. The directional impulse response is described as a sum of clusters (cf. [69]). Each cluster consists of up to 18 delay taps (separated by at least 10 nanoseconds), and to each tap is assigned a DoA and a truncated Laplacian power azimuth spectrum with angular spread ranging from 20° to 40° (and similar for the DoD). The number of clusters ranges from 2 to 6 (these numbers were found based on measurement data), and the overall RMS delay spread varies between 0 (flat fading) and 150 nanoseconds.

For any time instant, each MIMO channel tap is modeled by (14). For the Rayleigh-fading part, a Kronecker model is chosen. The Tx and Rx correlation matrices are determined by the power azimuth spectrum and by the array geometry; the latter can be specified by the user.

Time variations in the model are intended to emulate moving "environmental" scatterers. The prescribed Doppler spectrum consists of a "bell-shaped" part with low Doppler frequency and an optional additional peak at a larger Doppler frequency that corresponds to vehicles passing by. A special feature of the model are channel time-variations caused by fluorescent lights. This is taken into account by modulating several channel taps to artificially produce an amplitude modulation. As an additional option, polarization can be included.

4.5. SUI models and IEEE 802.16a

The so-called stanford university interim (SUI) channel models were developed for macrocellular fixed wireless access networks operating at 2.5 GHz and were further enhanced in the framework of the IEEE 802.16a standard [32]. The targeted scenario for these models is as follows:

(i) cell size is less than 10 km in radius;
(ii) user's antenna is fixed and installed under-the-eave or on rooftop (no line-of-sight is required);

(iii) base station height is 15 to 40 m, above rooftop level;
(iv) system bandwidth is flexible from 2 to 20 MHz.

The MIMO or directional component of the SUI/802.16a models is not highly developed within the standard itself, but extensions of the standard were investigated and are therefore described here as well.

4.5.1. SUI channel models

All six SUI tap-delay lines consist of three taps, and are valid for a distance between Tx and Rx equal to 7 km. The first tap is Ricean distributed for SUI channels 1 to 4, while all other taps are taken as Rayleigh fading. What should be emphasized is that each tap of any SUI channel is characterized by a single antenna correlation coefficient at the user's terminal (UT), irrespective of the UT array configuration, while the antenna correlation at the base station (BS) is taken as equal to zero, assuming a large BS antenna spacing. This is the only MIMO characteristic included in the model (no directional information is proposed). Note that in the original models, antennas were assumed to be omnidirectional at both sides. Another specific aspect of SUI models is that the Doppler spectrum of each tap is not given by the classical Jakes spectrum, but by a rounded shape centered around 0 Hz.

4.5.2. IEEE 802.16a channel models

IEEE 802.16a models are based on a modified version of the SUI channel models, valid for both omnidirectional and directional antennas. In the standard, the use of directional antennas naturally causes the K-factor of the Ricean taps to increase (the same holds true for the global narrowband K-factor) and the global delay-spread to decrease. However, the model does not modify the correlations at the UT when reducing the antenna beamwidth, although one might have expected the correlation coefficients to increase as the beamwidth decreases.

Additional features of the IEEE 802.16a standard include a pathloss model, a model for the narrowband Ricean K-factor, as well as an antenna gain reduction factor model (see [32] for more details). The path-loss model covers three terrain categories: hilly terrain with moderate-to-heavy tree densities (category A, to be used with SUI models 5 and 6), mostly flat terrain with light tree densities (category C, to be used with SUI models 1 and 2), and terrain with intermediate path loss condition, captured in category B (corresponding to SUI models 3 and 4).

4.5.3. 802.16a-based directional channel models

A spatial channel model based on the above standard has been developed in [61]. In fixed macrocellular scenarios, scattering mechanisms are mostly two-dimensional processes due to the narrow antenna elevation beamwidth at the base station. Hence, scatterers causing echoes with identical delays are situated on an ellipse with foci at the Tx and Rx locations. Consequently, any SUI tap-delay profile can be spatially represented by a GSCM using three ellipses, each one containing a specific number of scatterers, with the first ellipse degenerating to the link axis assuming LOS or quasi-LOS links. An advantage of the GSCM representation is the possibility to scale the Tx-Rx distance to other ranges (as the SUI models are only valid for a distance of 7 km). Furthermore, in order to match a desired correlation coefficient (at the terminal antenna side) for a typical half-wavelength spacing, the model in [61] makes use of a circular ring surrounding the terminal and bearing a subset of given scatterers taken among the estimated number of scatterers on the first ellipse. The so-called local scattering ratio (LSR) is defined as the ratio between the amount of local scatterers to the total amount of scatterers corresponding to the first ellipse (i.e., summing those on the local ring and those situated along the link axis). The LSR is therefore directly related to the scattering richness and the correlation coefficient. Finally, a further extension accounting for polarization is detailed in [89].

5. KEY FEATURES NOT INCLUDED IN PRESENT MODELS

As described in the foregoing sections, significant advances in the area of MIMO channel and propagation modeling have been made. Nonetheless, there are still a number of effects known from measurements that are not reliably reflected in existing models. Some of these features lacking in current models will be discussed next.

5.1. Single versus double scattering

Many geometry-based MIMO channel models assume single-bounce scattering between Tx and Rx. Diffraction and multiple-bounced scattering are often neglected, however. This implies a direct coupling of DoAs and DoDs and a joint Tx and Rx angular power spectrum that is not separable. Double-bounce scattering is also important for MIMO system performance.

Multiple-bounce scattering is physically more likely than single-bounce but does not necessarily lead to separable DoAs and DoDs.

Another aspect of existing models is that they assume that waves propagate equally likely between any pair of BS and MS scatterers [90]. This again implies that the angular power spectra at the Tx and Rx are separable.

5.2. Keyhole effect

If the distance between BS and MS is much larger than the BS and MS scatterer radius, this may lead to a small rank of the MIMO matrix and to different amplitude statistics; for all BS scatterers, the MS scatterers appear effectively as a single point source with Rayleigh amplitude statistics. These statistics multiply the usual Rayleigh distribution that results from the large number of MS scatterers.

A theoretical analysis revealed that for rank-one MIMO channel matrices the channel capacity is quite low (i.e., comparable to the capacity of single-antenna systems) [91]. Such channels have been termed "keyhole channels." A slightly

broader concept of rank-reduced channels, termed "pinhole" channels, was introduced in [90].

However, the identification of corresponding real-world propagation scenarios and the measurement of rank-reduced channels has been found to be extremely difficult [92]. An analytical model has been proposed [90] that is applicable for these type of channels and is essentially a modification of the Kronecker model obtained by inserting a low-rank scatterer correlation matrix in between the Tx and Rx correlation matrices. However, physical and geometry-based models up to now do not reproduce keyhole (pinhole) effects.

5.3. Diffuse multipath components

Geometry-based approaches usually model the radio channel via the superposition of a finite number of (specular) propagation paths (e.g., [14, 68]) that are typically characterized by their temporal and spatial statistics (these statistics usually are derived from channel measurements). The model accuracy can be controlled within certain limits via the number of propagation paths. However, it is not reasonable to increase the number of propagation paths beyond a certain threshold since this would result in over modeling and in difficulties to estimate the associated statistics reliably. For this reason, it has been proposed [93] to include an additional component into the model to describe nonspecular contributions, termed dense or diffuse MPCs. This extension is motivated by numerous measurements that showed that the channel impulse response consists of several well-concentrated strong paths (specular MPCs) and a huge number of weak paths (dense or diffuse MPCs). Many current models, however, are not able to reproduce diffuse MPCs reliably.

5.4. Polarization

Although dual-polarized arrays can be made smaller than single-polarized arrays and offer twice as much modes, polarization has attracted surprisingly little attention in MIMO channel modeling. To include polarization, each propagation path has to be described in terms of two orthogonal polarization states. Furthermore, depolarization caused by reflections, diffractions, and scattering turns two incoming states into four outgoing polarization states. A first geometry-based model for dual-polarized MIMO systems has been recently introduced in [89], describing each scatterer by means of a matrix coefficient with correlated random entries. In the 802.11 TGn model, depolarization is only modeled in a statistical fashion and the cross polarization ratio is treated as a random variable. Another difficulty in modeling polarization is the choice of the coordinate system (environment coordinates, Tx array/polarization coordinates, and Rx array/polarization coordinates) that can have a significant impact on the model complexity.

5.5. Time variation

Channel time variation is due to movement of terminals or scatterers. In the MIMO context, little experimental results have been obtained regarding time-variations, partly because of limitations in channel sounding equipment. Usually, only short-term variations (small-scale fading) and long-term variations (large-scale fading) are distinguished (cf. Section 1.5), although the physical causes for time-variations are much more diverse.

Analytical models tend to neglect these actual physical causes and capture any type of time-variations via statistical characterizations. Further measurements and experimental evidence is required to see whether this is indeed justified.

Deterministic, ray-tracing-based models or GSCMs can include channel time variations explicitly by prescribing Tx, Rx, or scatterer motion [18] (which itself will be characterized statistically). This will automatically reproduce realistic temporal correlations for successive channel snapshots.

In summary, both for physical and analytical channel models, much more conclusive measurements will be needed to incorporate time variance into MIMO channel models in a realistic fashion.

6. SUMMARY

This paper provided a survey of the most important concepts in channel and radio propagation modeling for wireless MIMO systems. We advocated an intuitive classification into physical models that focus on double-directional propagation and analytical models that concentrate on the channel impulse response (including antenna properties). For both model types, we reviewed popular examples that are widely used for the design and evaluation of MIMO systems. Furthermore, the most important features of a number of channel models proposed in the context of recent wireless standards were summarized. Finally, we discussed some open problems relating to channel features not sufficiently reproduced by current channel models.

Open problems are the parameterization of appropriate models for emerging new scenarios, like outdoor-to-indoor, and distributed MIMO networks. Significantly, more effort is necessary to validate channel models and to determine the applicability of the models in different environments.

ACKNOWLEDGMENT

This work was conducted within the EC funded Network-of-Excellence for Wireless Communications (NEWCOM).

REFERENCES

[1] E. Telatar, "Capacity of multi-antenna Gaussian channels," *European Transactions on Telecommunications*, vol. 10, no. 6, pp. 585–595, 1999.

[2] G. J. Foschini and M. J. Gans, "On limits of wireless communications in a fading environment when using multiple antennas," *Wireless Personal Communications*, vol. 6, no. 3, pp. 311–335, 1998.

[3] http://www.airgonetworks.com.

[4] http://www.beceem.com.

[5] http://world.belkin.com.

[6] http://www.broadcom.com.
[7] A. F. Molisch, *Wireless Communications*, Wiley-IEEE Press, New York, NY, USA, 2005.
[8] T. Rappaport, *Wireless Communications, Principles and Practice*, Prentice-Hall, Englewood Cliffs, NJ, USA, 1996.
[9] A. Paulraj, R. Nabar, and D. Gore, *Introduction to Spate-Time Wireless Communications*, Cambridge University Press, Cambridge, UK, 2003.
[10] L. Correia, Ed., *Mobile Broadband Multimedia Networks*, John Wiley & Sons, New York, NY, USA, 2006.
[11] http://www.lx.it.pt/cost273.
[12] M. Steinbauer, A. F. Molisch, and E. Bonek, "The double-directional radio channel," *IEEE Antennas and Propagation Magazine*, vol. 43, no. 4, pp. 51–63, 2001.
[13] M. Steinbauer, "The radio propagation channel—a non-directional, directional, and double-directional point-of-view," Ph.D. dissertation, Vienna University of Technology, Vienna, Austria, 2001.
[14] M. Steinbauer, "A comprehensive transmission and channel model for directional radio channel," in COST 259 TD (98) 027, Bern, Switzerland, February 1998.
[15] M. Steinbauer, D. Hampicke, G. Sommerkorn, et al., "Array measurement of the double-directional mobile radio channel," in *Proceedings of the 51st IEEE Vehicular Technology Conference (VTC '00)*, vol. 3, pp. 1656–1662, Tokio, Japan, May 2000.
[16] D. Asztély, B. Ottersten, and A. L. Swindlehurst, "Generalised array manifold model for wireless communication channels with local scattering," *IEE Proceedings - Radar, Sonar and Navigation*, vol. 145, no. 1, pp. 51–57, 1998.
[17] A. F. Molisch, H. Asplund, R. Heddergott, M. Steinbauer, and T. Zwick, "The COST 259 directional channel modelÂ—I: overview and methodology," *IEEE Transactions on Wireless Communications*, vol. 5, no. 12, pp. 3421–3433, 2006.
[18] L. M. Correia, Ed., *Wireless Flexible Personalised Communications (COST 259 Final Report)*, John Wiley & Sons, Chichester, UK, 2001.
[19] H. Özcelik, "Indoor MIMO channel models," Ph.D. dissertation, Institut für Nachrichtentechnik und Hochfrequenztechnik, Vienna University of Technology, Vienna, Austria, 2004, http://www.nt.tuwien.ac.at/mobile/theses finished.
[20] J. W. Wallace and M. A. Jensen, "Statistical characteristics of measured MIMO wireless channel data and comparison to conventional models," in *Proceedings of the 54th IEEE Vehicular Technology Conference (VTC '01)*, vol. 2, pp. 1078–1082, Sidney, Australia, October 2001.
[21] J. W. Wallace and M. A. Jensen, "Modeling the indoor MIMO wireless channel," *IEEE Transactions on Antennas and Propagation*, vol. 50, no. 5, pp. 591–599, 2002.
[22] A. Burr, "Capacity bounds and estimates for the finite scatterers MIMO wireless channel," *IEEE Journal on Selected Areas in Communications*, vol. 21, no. 5, pp. 812–818, 2003.
[23] M. Debbah and R. R. Müller, "MIMO channel modeling and the principle of maximum entropy," *IEEE Transactions on Information Theory*, vol. 51, no. 5, pp. 1667–1690, 2005.
[24] A. M. Sayeed, "Deconstructing multiantenna fading channels," *IEEE Transactions on Signal Processing*, vol. 50, no. 10, pp. 2563–2579, 2002.
[25] C.-N. Chuah, J. M. Kahn, and D. Tse, "Capacity of multi-antenna array systems in indoor wireless environment," in *Proceedings of IEEE Global Telecommunications Conference (GLOBECOM '98)*, vol. 4, pp. 1894–1899, Sidney, Australia, November 1998.
[26] D. Chizhik, F. Rashid-Farrokhi, J. Ling, and A. Lozano, "Effect of antenna separation on the capacity of BLAST in correlated channels," *IEEE Communications Letters*, vol. 4, no. 11, pp. 337–339, 2000.
[27] D.-S. Shiu, G. J. Foschini, M. J. Gans, and J. M. Kahn, "Fading correlation and its effect on the capacity of multielement antenna systems," *IEEE Transactions on Communications*, vol. 48, no. 3, pp. 502–513, 2000.
[28] J. P. Kermoal, L. Schumacher, K. I. Pedersen, P. E. Mogensen, and F. Frederiksen, "A stochastic MIMO radio channel model with experimental validation," *IEEE Journal on Selected Areas in Communications*, vol. 20, no. 6, pp. 1211–1226, 2002.
[29] W. Weichselberger, M. Herdin, H. Özcelik, and E. Bonek, "A stochastic MIMO channel model with joint correlation of both link ends," *IEEE Transactions on Wireless Communications*, vol. 5, no. 1, pp. 90–99, 2006.
[30] 3GPP - 3GPP2 Spatial Channel Model Ad-hoc Group3GPP TR 25.996, "Spatial Channel Model for Multiple Input Multiple Output (MIMO) Simulations," v6.1.0 (2003-09).
[31] http://www.ist-winner.org/.
[32] V. Erceg, K. V. S. Hari, M. S. Smith, et al., "Channel models for fixed wireless applications," Contribution IEEE 802.16.3c-01/29r4, IEEE 802.16 Broadband Wireless Access Working Group.
[33] V. Erceg, L. Schumacher, P. Kyritsi, et al., "TGn channel models," Tech. Rep. IEEE P802.11, Wireless LANs, Garden Grove, Calif, USA, 2004, http://www.802wirelessworld.com/8802.
[34] P. Bello, "Characterization of randomly time-variant linear channels," *IEEE Transactions on Communications*, vol. 11, no. 4, pp. 360–393, 1963.
[35] R. Vaughan and J. B. Andersen, *Channels, Propagation and Antennas for Mobile Communications*, IEE Press, London, UK, 2003.
[36] R. Kattenbach, "Considerations about the validity of WSSUS for indoor radio channels," in *COST 259 TD(97)070, 3rd Management Committee Meeting*, Lisbon, Portugal, September 1997.
[37] L. Dossi, G. Tartara, and F. Tallone, "Statistical analysis of measured impulse response functions of 2.0 GHz indoor radio channels," *IEEE Journal on Selected Areas in Communications*, vol. 14, no. 3, pp. 405–410, 1996.
[38] J. Kivinen, X. Zhao, and P. Vainikainen, "Empirical characterization of wideband indoor radio channel at 5.3 GHz," *IEEE Transactions on Antennas and Propagation*, vol. 49, no. 8, pp. 1192–1203, 2001.
[39] M. K. Tsatsanis, G. B. Giannakis, and G. Zhou, "Estimation and equalization of fading channels with random coefficients," *Signal Processing*, vol. 53, no. 2-3, pp. 211–229, 1996.
[40] G. Matz, "On non-WSSUS wireless fading channels," *IEEE Transactions on Wireless Communications*, vol. 4, no. 5, pp. 2465–2478, 2005.
[41] E. Biglieri, J. Proakis, and S. Shamai, "Fading channels: information-theoretic and communications aspects," *IEEE Transactions on Information Theory*, vol. 44, no. 6, pp. 2619–2692, 1998.
[42] A. M. Sayeed and B. Aazhang, "Joint multipath-Doppler diversity in mobile wireless communications," *IEEE Transactions on Communications*, vol. 47, no. 1, pp. 123–132, 1999.
[43] R. Bultitude, G. Brussaard, M. Herben, and T. J. Willink, "Radio channel modelling for terrestrial vehicular mobile applications," in *Proceedings of Millenium Conference on Antennas and Propagation*, pp. 1–5, Davos, Switzerland, April 2000.
[44] A. Gehring, M. Steinbauer, I. Gaspard, and M. Grigat, "Empirical channel stationarity in urban environments," in *Proceedings of the 4th European Personal Mobile Communications Conference (EPMCC '01)*, Vienna, Austria, February 2001.

[45] K. Hugl, "Spatial channel characteristics for adaptive antenna downlink transmission," Ph.D. dissertation, Vienna University of Technology, Vienna, Austria, 2002.

[46] I. Viering, H. Hofstetter, and W. Utschick, "Validity of spatial covariance matrices over time and frequency," in *Proceedings of IEEE Global Telecommunications Conference (GLOBECOM '02)*, vol. 1, pp. 851–855, Taipeh, Taiwan, November 2002.

[47] M. Herdin, "Non-stationary indoor MIMO radio channels," Ph.D. dissertation, Vienna University of Technology, Vienna, Austria, 2004.

[48] C. Balanis, *Advanced Engineering Electromagnetics*, John Wiley & Sons, New York, NY, USA, 1999.

[49] R. G. Kouyoumjian and P. H. Pathak, "A uniform geometrical theory of diffraction for an edge in a perfectly conducting surface," *Proceedings of the IEEE*, vol. 62, no. 11, pp. 1448–1461, 1974.

[50] R. J. Leubbers, "Finite conductivity uniform GTD versus knife edge diffraction in prediction of propagation path loss," *IEEE Transactions on Antennas and Propagation*, vol. 32, no. 1, pp. 70–76, 1984.

[51] H. Bertoni, *Radio Propagation for Modern Wireless Systems*, Prentice Hall PTR, Englewood Cliffs, NJ, USA, 2000.

[52] J. Ling, D. Chizhik, and R. A. Valenzuela, "Predicting multi-element receive & transmit array capacity outdoors with ray tracing," in *Proceedings of the 53rd IEEE Vehicular Technology Conference (VTC '01)*, vol. 1, pp. 392–394, Rhodes, Greece, May 2001.

[53] C. Cheon, G. Liang, and H. L. Bertoni, "Simulating radio channel statistics for different building environments," *IEEE Journal on Selected Areas in Communications*, vol. 19, no. 11, pp. 2191–2200, 2001.

[54] V. Degli-Esposti, D. Guiducci, A. de'Marsi, P. Azzi, and F. Fuschini, "An advanced field prediction model including diffuse scattering," *IEEE Transactions on Antennas and Propagation*, vol. 52, no. 7, pp. 1717–1728, 2004.

[55] W. Lee, "Effect on correlation between two mobile radio base-station antennas," *IEEE Transactions on Communications*, vol. 21, no. 11, pp. 1214–1224, 1973.

[56] P. Petrus, J. H. Reed, and T. S. Rappaport, "Geometrical-based statistical macrocell channel model for mobile environments," *IEEE Transactions on Communications*, vol. 50, no. 3, pp. 495–502, 2002.

[57] J. C. Liberti and T. S. Rappaport, "A geometrically based model for line-of-sight multipath radio channels," in *Proceedings of the 46th IEEE Vehicular Technology Conference (VTC '96)*, vol. 2, pp. 844–848, Atlanta, Ga, USA, April-May 1996.

[58] J. J. Blanz and P. Jung, "A flexibly configurable spatial model for mobile radio channels," *IEEE Transactions on Communications*, vol. 46, no. 3, pp. 367–371, 1998.

[59] O. Norklit and J. B. Andersen, "Diffuse channel model and experimental results for array antennas in mobile environments," *IEEE Transactions on Antennas and Propagation*, vol. 46, no. 6, pp. 834–840, 1998.

[60] J. Fuhl, A. F. Molisch, and E. Bonek, "Unified channel model for mobile radio systems with smart antennas," *IEE Proceedings - Radar, Sonar and Navigation*, vol. 145, no. 1, pp. 32–41, 1998, special issue on antenna array processing techniques.

[61] C. Oestges, V. Erceg, and A. J. Paulraj, "A physical scattering model for MIMO macrocellular broadband wireless channels," *IEEE Journal on Selected Areas in Communications*, vol. 21, no. 5, pp. 721–729, 2003.

[62] A. F. Molisch, A. Kuchar, J. Laurila, K. Hugl, and R. Schmalenberger, "Geometry-based directional model for mobile radio channels—principles and implementation," *European Transactions on Telecommunications*, vol. 14, no. 4, pp. 351–359, 2003.

[63] J. Laurila, A. F. Molisch, and E. Bonek, "Influence of the scatterer distribution on power delay profiles and azimuthal power spectra of mobile radio channels," in *Proceedings of the 5th International Symposium on Spread Spectrum Techniques & Applications (ISSSTA '98)*, vol. 1, pp. 267–271, Sun City, South Africa, September 1998.

[64] M. Toeltsch, J. Laurila, K. Kalliola, A. F. Molisch, P. Vainikainen, and E. Bonek, "Statistical characterization of urban spatial radio channels," *IEEE Journal on Selected Areas in Communications*, vol. 20, no. 3, pp. 539–549, 2002.

[65] H. Suzuki, "A statistical model for urban radio propagation," *IEEE Transactions on Communications*, vol. 25, no. 7, pp. 673–680, 1977.

[66] A. Kuchar, J.-P. Rossi, and E. Bonek, "Directional macro-cell channel characterization from urban measurements," *IEEE Transactions on Antennas and Propagation*, vol. 48, no. 2, pp. 137–146, 2000.

[67] C. Bergljung and P. Karlsson, "Propagation characteristics for indoor broadband radio access networks in the 5 GHz band," in *Proceedings of the 9th IEEE International Symposium on Personal, Indoor and Mobile Radio Communications (PIMRC '98)*, vol. 2, pp. 612–616, Boston, Mass, USA, September 1998.

[68] A. F. Molisch, "A generic model for MIMO wireless propagation channels in macro- and microcells," *IEEE Transactions on Signal Processing*, vol. 52, no. 1, pp. 61–71, 2004.

[69] A. A. M. Saleh and R. A. Valenzuela, "A statistical model for indoor multipath propagation," *IEEE Journal on Selected Areas in Communications*, vol. 5, no. 2, pp. 128–137, 1987.

[70] C.-C. Chong, C.-M. Tan, D. Laurenson, S. McLaughlin, M. A. Beach, and A. R. Nix, "A new statistical wideband spatio-temporal channel model for 5-GHz band WLAN systems," *IEEE Journal on Selected Areas in Communications*, vol. 21, no. 2, pp. 139–150, 2003.

[71] Q. H. Spencer, B. D. Jeffs, M. A. Jensen, and A. L. Swindlehurst, "Modeling the statistical time and angle of arrival characteristics of an indoor multipath channel," *IEEE Journal on Selected Areas in Communications*, vol. 18, no. 3, pp. 347–360, 2000.

[72] T. Zwick, C. Fischer, and W. Wiesbeck, "A stochastic multipath channel model including path directions for indoor environments," *IEEE Journal on Selected Areas in Communications*, vol. 20, no. 6, pp. 1178–1192, 2002.

[73] P. Soma, D. S. Baum, V. Erceg, R. Krishnamoorthy, and A. J. Paulraj, "Analysis and modeling of multiple-input multiple-output (MIMO) radio channel based on outdoor measurements conducted at 2.5 GHz for fixed BWA applications," in *Proceedings of IEEE International Conference on Communications (ICC '02)*, vol. 1, pp. 272–276, New York, NY, USA, April-May 2002.

[74] W. Weichselberger, "Spatial structure of multiple antenna radio channels," Ph.D. dissertation, Institut für Nachrichtentechnik und Hochfrequenztechnik, Vienna University of Technology, Vienna, Austria, 2003, http://www.nt.tuwien.ac.at/mobile/theses finished.

[75] D. McNamara, M. Beach, P. Fletcher, and P. Karlsson, "Initial investigation of multiple-input multiple-output channels in indoor environments," in *Proceedings of the IEEE Benelux Chapter Symposium on Communications and Vehicular Technology (SCVT '00)*, pp. 139–143, Leuven, Belgium, October 2000.

[76] E. Bonek, H. Özcelik, M. Herdin, W. Weichselberger, and J. Wallace, "Deficiencies of the 'Kronecker' MIMO radio channel model," in *Proceeding of the 6th International Symposium on*

Wireless Personal Multimedia Communications (WPMC '03), Yokosuka, Japan, October 2003.

[77] W. Jakes, *Microwave Mobile Communications*, IEEE Press, New York, NY, USA, 1974.

[78] S. Foo, M. Beach, and A. Burr, "Wideband outdoor MIMO channel model derived from directional channel measurements at 2 GHz," in *Proceedings of the 7th International Symposium on Wireless Personal Multimedia Communications (WPMC '04)*, Abano Terme, Italy, September 2004.

[79] K. Liu, V. Raghavan, and A. M. Sayeed, "Capacity scaling and spectral efficiency in wide-band correlated MIMO channels," *IEEE Transactions on Information Theory*, vol. 49, no. 10, pp. 2504–2526, 2003.

[80] M. Debbah, R. Müller, H. Hofstetter, and P. Lehne, "Validation of mutual information complying MIMO models," submitted to *IEEE Transactions on Wireless Communications*.

[81] M. Debbah and R. Müller, "Capacity complying MIMO channel models," in *Proceedings of the 37th Annual Asilomar Conference on Signals, Systems and Computers (ACSSC '03)*, vol. 2, pp. 1815–1819, Pacific Grove, Calif, USA, November 2003.

[82] A. F. Molisch, H. Hofstetter, et al., "The COST273 channel model," in *COST 273 Final Report*, L. Correia, Ed., Springer, New York, NY, USA, 2006.

[83] International Telecommunications Union, "Guidelines for evaluation of radio transmission technologies for imt-2000," Tech. Rep. ITU-R M.1225, The International Telecommunications Union, Geneva, Switzerland, 1997.

[84] D. S. Baum, J. Hansen, G. Del Galdo, M. Milojevic, J. Salo, and P. Kyösti, "An interim channel model for beyond-3G systems: extending the 3GPP spatial channel model (SCM)," in *Proceedings of the 61st IEEE Vehicular Technology Conference (VTC '05)*, vol. 5, pp. 3132–3136, Stockholm, Sweden, May-June 2005.

[85] H. El-Sallabi, D. Baum, P. Zetterberg, P. Kyösti, T. Rautiainen, and C. Schneider, "Wideband spatial channel model for MIMO systems at 5 GHz in indoor and outdoor environments," in *Proceedings of the 63rd IEEE Vehicular Technology Conference (VTC '06)*, vol. 6, pp. 2916–2921, Melbourne, Australia, May 2006.

[86] J. Medbo and J.-E. Berg, "Measured radio wave propagation characteristics at 5 GHz for typical HIPERLAN/2 scenarios," Tech. Rep. 3ERI074a, ETSI, Sophia-Antipolis, France, 1998.

[87] J. Medbo and P. Schramm, "Channel models for HIPERLAN/2," Tech. Rep. 3ERI085B, ETSI, Sophia-Antipolis, France, 1998.

[88] L. Schumacher, "WLAN MIMO channel matlab program," http://www.info.fundp.ac.be/~lsc/Research/IEEE_80211_HTSG_CMSC/distribution_terms.html.

[89] C. Oestges, V. Erceg, and A. Paulraj, "Propagation modeling of multi-polarized MIMO fixed wireless channels," *IEEE Transactions on Vehicular Technology*, vol. 53, no. 3, pp. 644–654, 2004.

[90] D. Gesbert, H. Bölcskei, D. A. Gore, and A. J. Paulraj, "Outdoor MIMO wireless channels: models and performance prediction," *IEEE Transactions on Communications*, vol. 50, no. 12, pp. 1926–1934, 2002.

[91] D. Chizhik, G. Foschini, M. Gans, and R. Valenzuela, "Keyholes, correlations, and capacities of multielement transmit and receive antennas," *IEEE Transactions on Wireless Communications*, vol. 1, no. 2, pp. 361–368, 2002.

[92] P. Almers, F. Tufvesson, and A. F. Molisch, "Measurement of keyhole effect in a wireless multiple-input multiple-output (MIMO) channel," *IEEE Communications Letters*, vol. 7, no. 8, pp. 373–375, 2003.

[93] A. Richter, C. Schneider, M. Landmann, and R. Thomä, "Parameter estimation results of specular and dense multipath components in micro-cell scenarios," in *Proceedings of the 7th International Symposium on Wireless Personal Multimedia Communications (WPMC '04)*, Abano Terme, Italy, September 2004.